

# Signature of primordial non-Gaussianity on large scale structure

Tsz Yan Lam (IPMU, U of Tokyo)

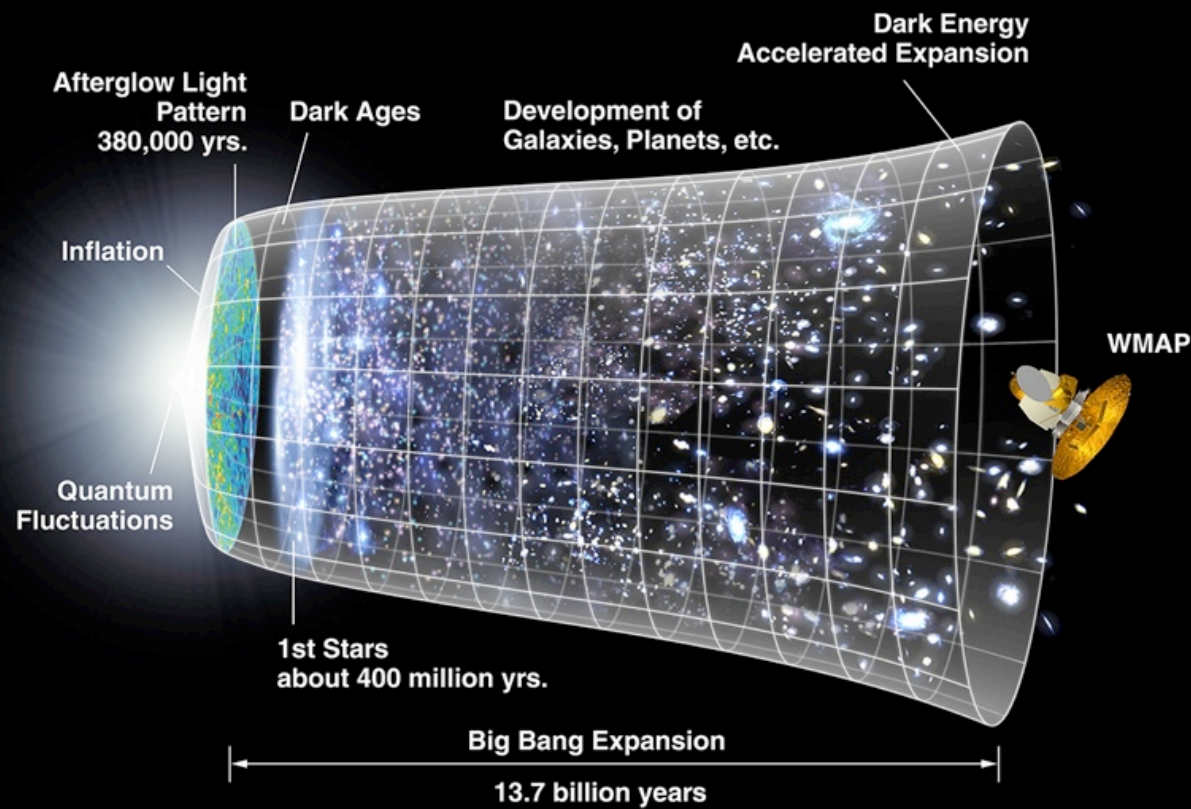
with Ravi K. Sheth (UPenn) and Vincent Desjacques (U of Zurich)

# Primordial non-Gaussianity

- \* Why study primordial non-Gaussianity?
- \* The most common single (scalar) field, slow-roll inflation predicts the primordial perturbation to be Gaussian.
- \* Detections of primordial non-Gaussianity can constrain inflation models.
- \* Local  $f_{nl}$  model:

$$\Phi = \phi_g + f_{nl}(\phi_g^2 - \langle \phi_g^2 \rangle)$$

# A brief history of the Universe



NASA/WMAP Science team

NASA/WMAP Science Team

# Signatures of Primordial non-Gaussianity

- \* Modification in the primordial perturbation left signatures on CMB and LSS
- \* Some debates on the current constraints on  $f_{nl}$  from CMB:
- \* Yadav & Wandelt (2008):  $27 < f_{nl} < 147 - 3\sigma$  detection
- \* Komatsu et al. (2009):  $-9 < f_{nl} < 111$
- \* Using LSS to constrain  $f_{nl}$
- \* difficulties: gravitational evolution transforms a Gaussian distribution to a non-Gaussian one AND
- \* the non-Gaussianity from gravitational evolution is much stronger than the primordial contribution

# Signature of Primordial non-Gau on LSS

- \* power spectrum and bi-spectrum (Scoccimarro, Sefusatti & Zaldarriaga 2004);
- \* scale dependent halo bias (Dalal et al. 2008; Slosar et al. 2008);
- \* PDF of dark matter field
- \* halo mass function (Verde et al. 2008; TYL & Sheth 2009; TYL, Sheth & Desjacques 2009);
- \* redshift space distortion
- \* halo mass function
- \* probability distribution of dark matter field
- \* void abundances (Grossi et al. 2008; TYL & Sheth 2009; TYL, Desjacques & Sheth 2009);
- \* void abundances (Kamionkowski, Verde & Jimenez 2009; TYL, Sheth & Desjacques 2009);
- \* weak lensing mass map of high z galaxy cluster (Jimenez & Verde 2009)

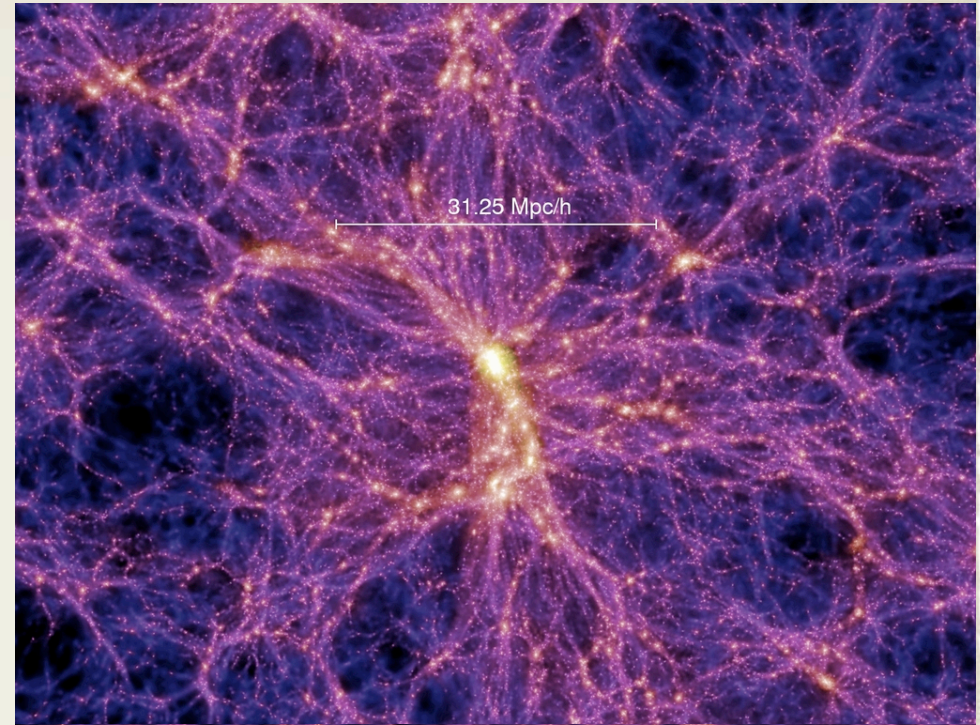
# PDF of dark matter field

\* PDF of dark matter field  
--  $p(M|V)$  measure the probability of having mass  $M$  in volume  $V$

\* gravitational instability causes overdense region to collapse and underdense region to expand  $\longrightarrow$

the resulting distribution is highly non-gaussian

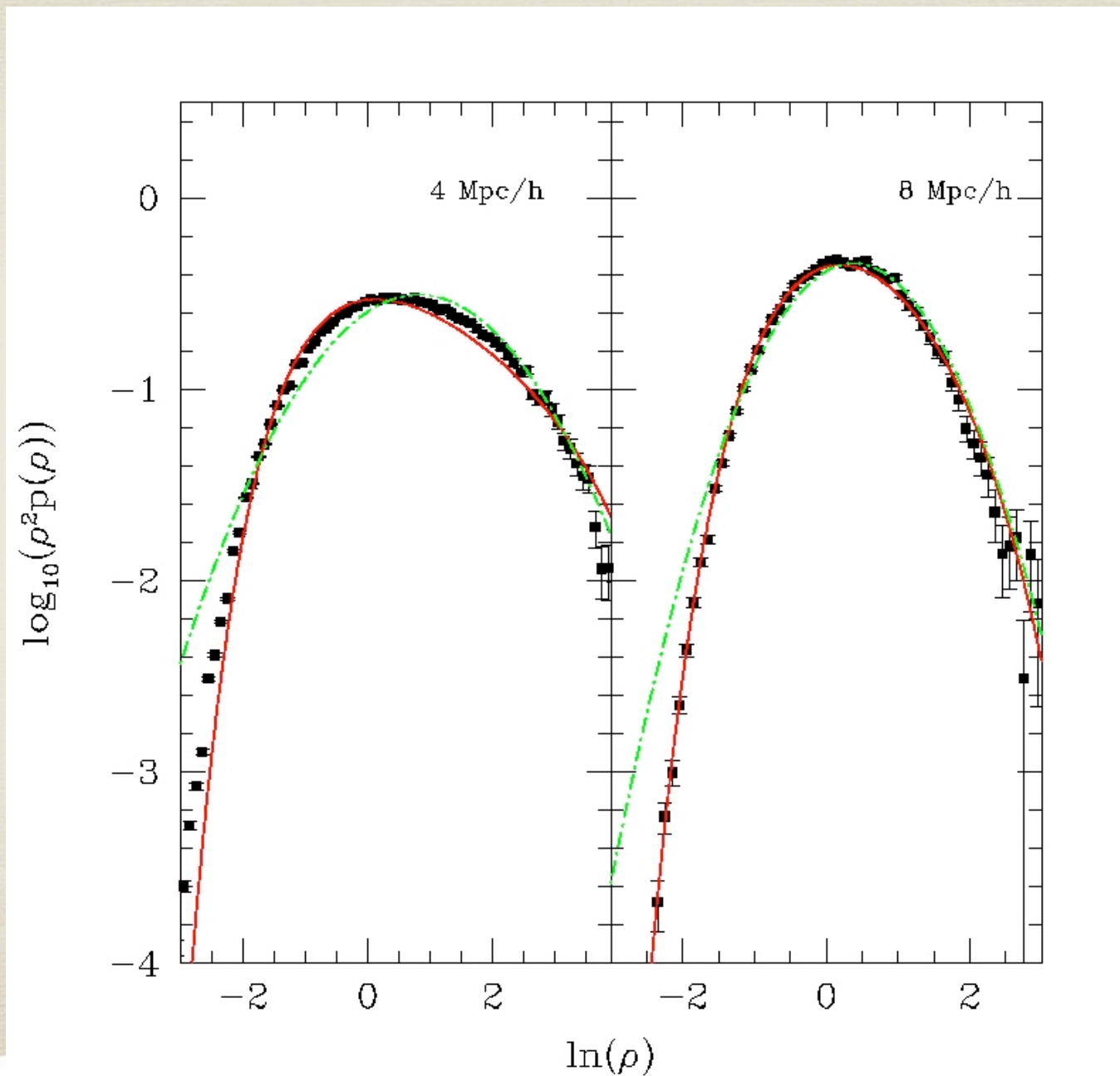
\* provides foundation to study the distributions of bias tracers (halos, galaxies and 21 cm)



$z=5.8$  (14.6 Gyr)

MPA (Garching)

# PDF of dark matter field for $f_{nl} = 0$



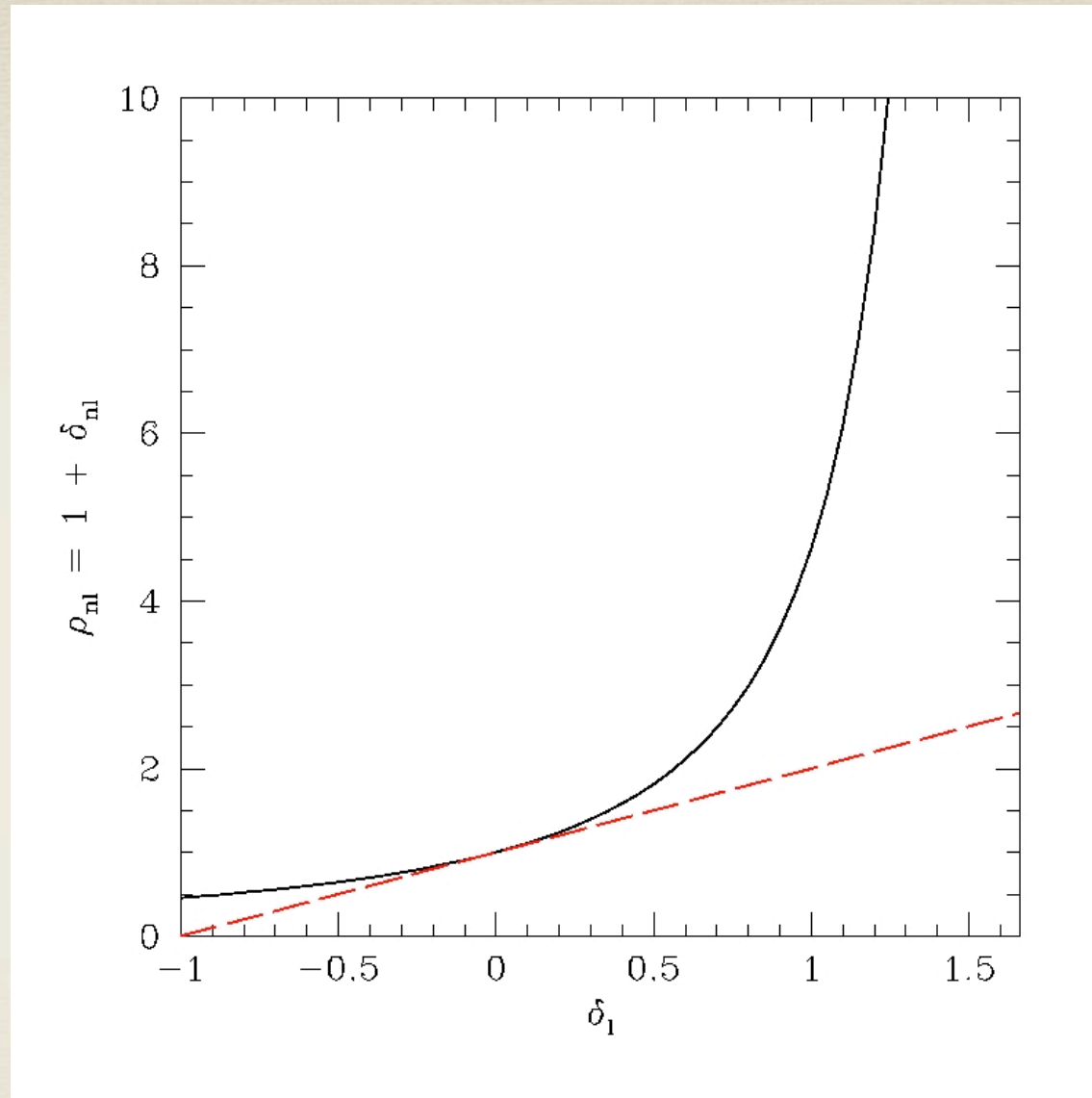
# Spherical collapse model

- \* Assume the gravitational evolution is spherical symmetric: there exists a 1-1 mapping to predict the nonlinear overdensity  $\delta_{\text{NL}}$  from the linear overdensity  $\delta_l$

$$\rho \equiv 1 + \delta_{\text{NL}} = \frac{M}{\bar{\rho}V} = \left(1 - \frac{\delta_l}{\delta_c}\right)^{-\delta_c}$$

(Bernardeau 1994; Sheth 1998) where  $\delta_c = 1.66$  for  $\Lambda$ CDM universe

Source: Florida Center for Instructional Technology Clipart  
(Tampa: University of South Florida, 2007)



- \*  $\rho_{nl} = 1 + \delta_{nl} \approx 1 + \delta_l$  when  $\delta_l \sim 0$ .
- \*  $\rho_{nl}$  diverges as  $\delta_l \rightarrow \delta_c$

## PDF of dark matter field

- \* Given the linear-nonlinear mapping (spherical collapse model), what we need is a statistical method to relate the two distributions  $p(\delta_l)$  and  $p(\delta_{\text{NL}}|V) = p(\rho|V)$
- \* TYL & Sheth (2008) showed that the local deterministic perturbation theory approach fares well compared to more complicated excursion set approach (which includes the cloud-in-cloud effect)

$$\int_M^\infty dM' p(M'|V) \frac{M'}{\bar{M}} = \int_{\delta_l(M,V)}^\infty d\delta p(\delta|M, V)$$

extra weighting factor

Note: the correct smoothing scale in the initial field = volume containing the mass  $M$

## PDF of DM field (Initial distribution)

- \* When the initial perturbation is described by Gaussian distribution, the distribution on rhs is given by

$$p(x)dx = \frac{e^{-x^2/2}}{\sqrt{2\pi}} dx \quad \text{where } x = \frac{\delta_l}{\sigma(M)}$$

- \* For non zero  $f_{nl}$ , approximate the distribution by Edgeworth expansion:

$$p(\delta_l|R_l)d\delta_l = \frac{e^{-\nu^2(R_l)/2}}{\sqrt{2\pi}} \left[ 1 + \frac{\sigma_{NG}(R_l)S_3(R_l)}{6} H_3(\nu(R_l)) + \dots \right] d\nu(R_l)$$

where  $\nu(R_l) = \delta_l/\sigma_{NG}(R_l)$   $H_3(\nu) = \nu(nu^2 - 3)$

$$S_3 = \langle \delta_l^3 \rangle / \sigma_{rmNG}^4 \quad \sigma_{NG} = \langle \delta_l^2 \rangle$$

and terms higher than  $S_3(R_l)$  are neglected

# Nonlinear PDF in real space

- \* With the initial distribution, the nonlinear pdf can be computed:

$$\rho^2 p(\rho|V) = p_{\text{NG}}(\delta_l(\rho)|V_l(\rho)) \nu \frac{d \ln \nu}{d \ln \rho}$$

- \* Hence its functional form is:

$$\begin{aligned} \rho^2 p(\rho|V) &= \frac{1}{\sqrt{2\pi\sigma^2(\rho)}} \exp\left[-\frac{\delta_l^2(\rho)}{2\sigma^2(\rho)}\right] \left[1 + \frac{\sigma S_3(\rho)}{6} H_3\left(\frac{\delta_l(\rho)}{\sigma(\rho)}\right)\right] \\ &\quad \times \left[1 - \frac{\delta_l(\rho)}{\delta_c} + \frac{\gamma_\sigma}{6} \delta_l(\rho)\right] \\ &= \rho^2 p_G(\rho|V) \left[1 + \frac{\sigma S_3(\rho)}{6} H_3\left(\frac{\delta_l(\rho)}{\sigma(\rho)}\right)\right] \end{aligned}$$

modifications due to primordial non-Gaussianity

## Modification factor in real space PDF

$$\left[ 1 + \frac{\sigma S_3(\rho)}{6} H_3 \left( \frac{\delta_l(\rho)}{\sigma(\rho)} \right) \right]$$

\*  $\sigma S_3 = 0$  when  $f_{nl} = 0 \rightarrow$  returns to Gaussian results

\*  $\delta_l = 0$  when  $\rho = 1 \rightarrow$  little or no correction near  $\rho \approx 1$

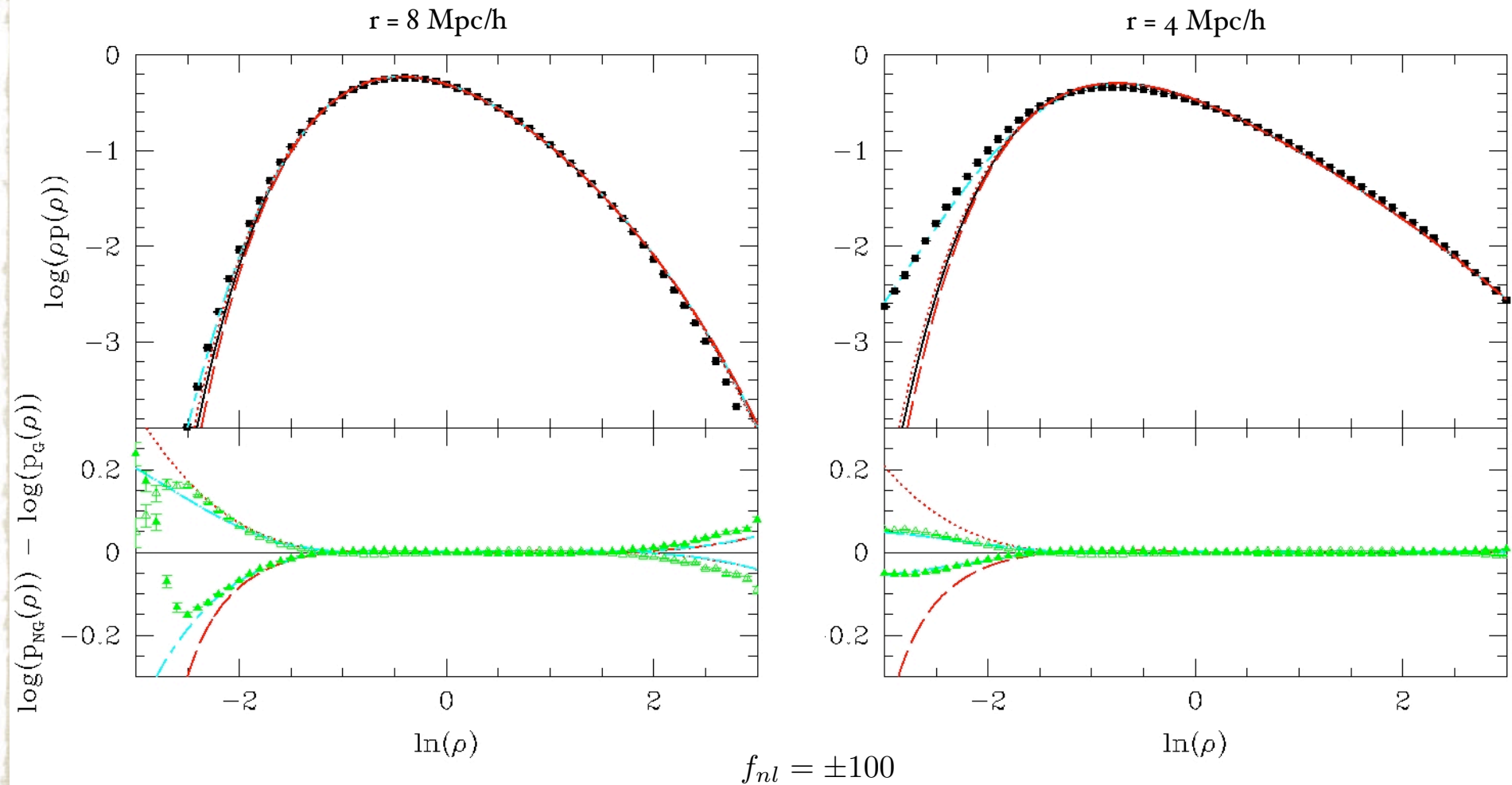
\* For typical value of  $\gamma_\sigma (\approx 6/5)$ , one find the following:

$$\begin{aligned} H_3 &\propto \rho^{3/5} \text{ for } \rho \gg 1 \\ &\propto -\rho^{6/5} \text{ for } \rho \ll 1 \end{aligned}$$

Contrary to the change in the initial distribution the modification in the nonlinear PDF is asymmetric  $\longrightarrow$

the effect is expected to be stronger in the underdense region

# Comparisons to N-body measurements

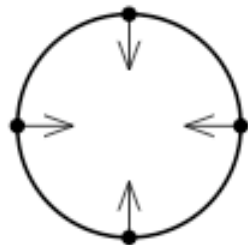


## Signature on redshift space distortion

- \* Our model successfully describes the signature of primordial non-Gaussianity in the real space PDF.
- \* Note that, however, observations are made in redshift space coordinate.
- \* Non zero  $f_{nl}$  in the primordial perturbation also affects both the matter and velocity distributions. Hence modification in redshift space distortion is expected.

# Redshift space distortion

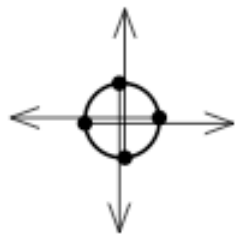
Real space:



Linear regime



Turnaround



Collapsing

Redshift space:



Squashing effect



Collapsed



Finger-of-god

Hamilton 1997

## Redshift space distortion when $f_{nl} = 0$

- \* The redshift space density power spectrum is related to the real space density power spectrum:

$$P_s(\mathbf{k}) = (1 + f\mu^2)^2 P(k)$$

where  $\mu = \cosine$  of the angle to the line of sight

and  $f \approx \Omega_m^{0.6}$

- \* The average over  $\mu$  gives the well-known Kaiser formula:

$$\left(1 + \frac{2}{3}f + \frac{1}{5}f^2\right)$$

## Redshift space distortion for non zero $f_{nl}$

- \* In this talk I will use the ellipsoidal collapse model to compute the redshift space distortion for the case when  $f_{nl}$  is non zero.
- \* Ellipsoidal collapse model is an approximation which describes the gravitational evolution tri-axially.
- \* It reduces to perturbation theory at early time (Bond & Myers 1996), but allows one to study more nonlinear structure (Sheth et al. 2001; Desjacques 2008).
- \* Ohta et al. (2004) and TYL & Sheth (2008) showed that when  $f_{nl}$  is zero, the ellipsoidal collapse predicts the Kaiser formula.

## Ingredients for ellipsoidal collapse

- \* Ellipsoidal collapse model requires the knowledge of the distribution of the eigenvalues of the shear field;
- \* When  $f_{nl} = 0$  it is given by the Doroshkevich celebrated formula.
- \* The extension to the local  $f_{nl}$  model is given by TYL, Sheth & Desjacques (2009).
- \* Denote  $\lambda_i$  as the eigenvalues of the initial shear field which is proportional to  $\Phi_{ij}$ , where

$$\Phi_{ij} = \phi_{ij} + 2f_{nl}(\phi_i\phi_j + \phi\phi_{ij})$$

\* The correlations of  $\Phi_{ij}$  are important: we want to find a set of independent elements of the shear field components.

\* It turns out that the three off-diagonal components are not correlated.

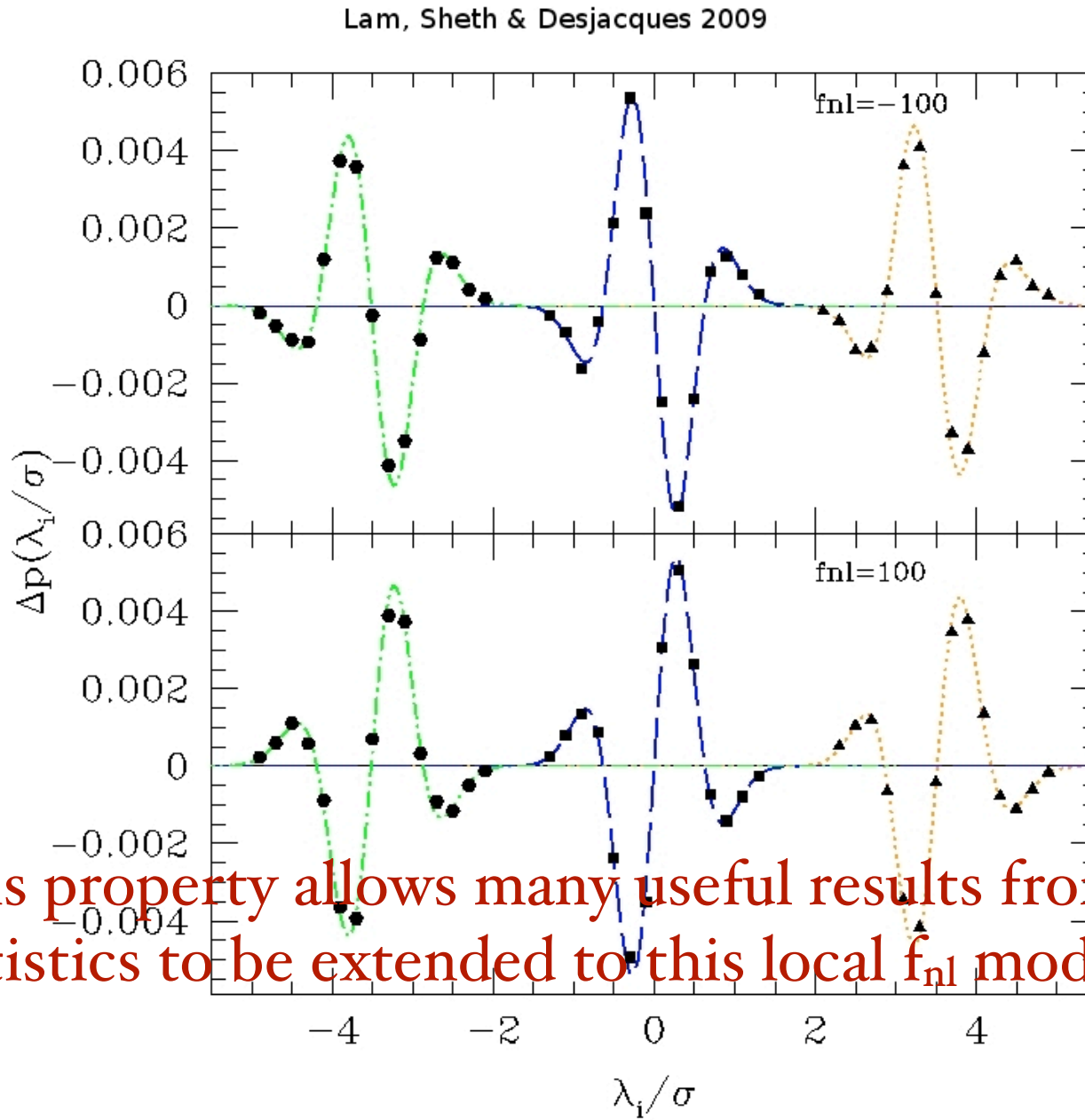
\* The three diagonal components are correlated. Define

$$x = \sum_i \Phi_{ii} \quad y = \frac{1}{2}(\Phi_{11} - \Phi_{22}) \quad z = \frac{1}{2}(\Phi_{11} + \Phi_{22} - 2\Phi_{33})$$

\* The new set  $\{x, y, z, \Phi_{12}, \Phi_{23}, \Phi_{31}\}$  forms an independent set.

\* Five of the six components (except  $x$ ) have zero skewness up to second order of  $f_{nl}$   $\longrightarrow$  those are drawn from Gaussian distributions.

- \* No
- he
- wh
- exp
- \* Th
- \*  $p(\lambda_i/\sigma)$



This property allows many useful results from Gaussian statistics to be extended to this local  $f_{n1}$  model easily

or,  
l,  
worth

$H_3(\delta_l/\sigma)$

## Ellipsoidal collapse model

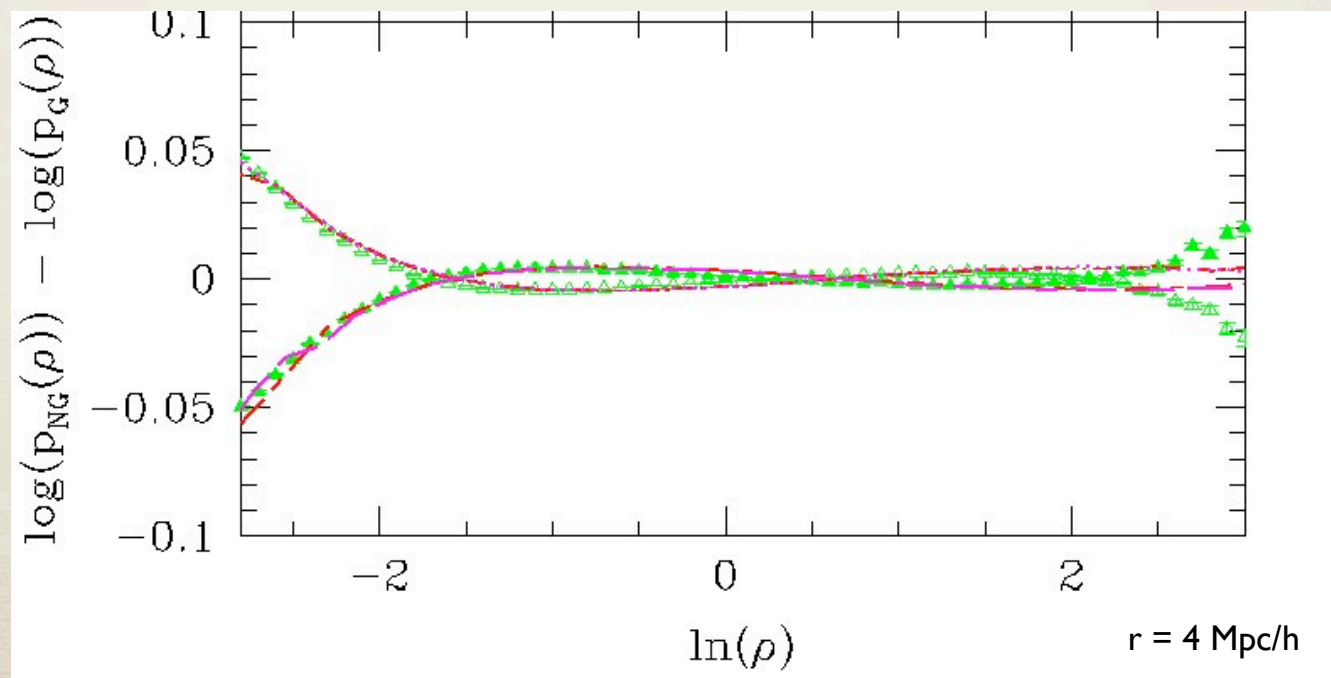
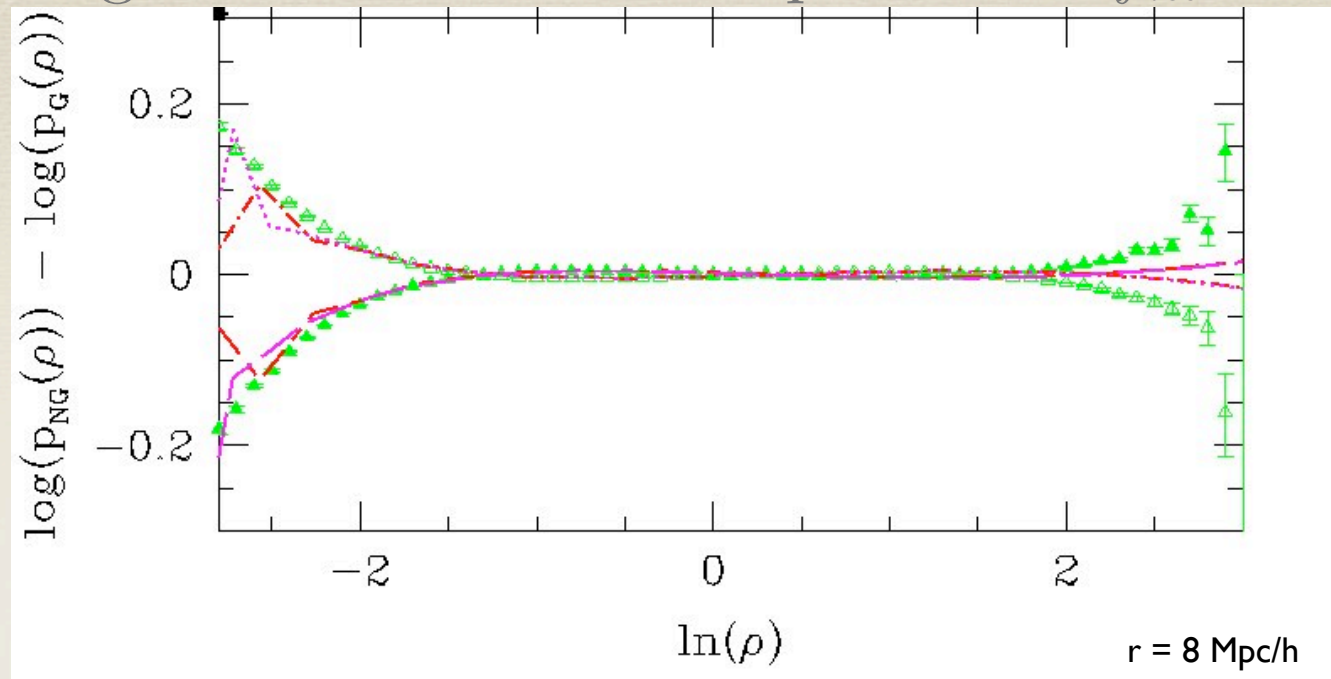
- \* TYL & Sheth (2008) derived an improved approximation of the ellipsoidal collapse model: can be viewed as combining the Zeldovich approximation and the spherical collapse model.

$$\rho_r = \frac{(1 - \delta_l/3)^3}{(1 - \delta_l/\delta_c)^{\delta_c}} \prod_{j=1}^3 (1 - \lambda_j)^{-1}$$

where  $\delta_c \approx 1.66$  and  $\delta_l = \sum_i \lambda_i$

- \* When all  $\lambda_i$  are equal, the above expression returns to the spherical collapse approximation.
- \* The correction factor compared to the Zeldovich approximation is the ratio of a Zeldovich sphere to the “exact” spherical solution.

# Change in the distribution profile for $f_{nl} = \pm 100$



## Kaiser factor from ellipsoidal collapse model

- \* Kaiser factor can be derived by expanding the ellipsoidal collapse in series form:

$$1 + \delta_s = 1 + \delta_s^{(1)} + \delta_s^{(2)} + \delta_s^{(3)} + \dots$$

where  $\delta_s^{(1)} = \delta_r^{(1)} + \Delta_z^{(1)}$

$$\delta_s^{(2)} = \delta_r^{(2)} + \Delta_z^{(2)} + \delta_r^{(1)} \Delta_z^{(1)}$$

$$\delta_s^{(3)} = \delta_r^{(3)} + \Delta_z^{(3)} + \delta_r^{(2)} \Delta_z^{(1)} + \delta_r^{(1)} \Delta_z^{(2)}$$

- \* The variance can be computed by taking the average over the distribution of  $\lambda$ ;
- \* Non zero  $f_{nl}$  only changes the values of the averages.

## Signature of $f_{nl}$ on redshift space distortion

- \* The Kaiser factor can be derived by looking at the variance of the dark matter fluctuation.
- \* The zeroth order gives the ordinary Kaiser factor and it is independent of  $f_{nl}$ :

$$\langle \delta_s^2 \rangle \approx \langle (\delta_r^{(1)})^2 \rangle = \left( 1 + \frac{2}{3} f_1 + \frac{1}{5} f_1^2 \right) \sigma^2$$

$\swarrow P_{\delta\delta}$                        $\nwarrow P_{\delta v}$                        $\swarrow P_{vv}$

- \* Signature of primordial non-Gaussianity is in the first order correction:

$$\langle \delta_s^2 \rangle^{(2)} = 2 \frac{\sigma S_3}{6} \sigma^3 \left[ 3\nu_2 + \left( \nu_2 + \frac{2}{3} \right) f_1 - \frac{44}{45} f_1^2 + \frac{4}{9} f_1^3 + \frac{\nu_2}{3} f_1 f_2 + \nu_2 f_2 \right]$$

$\nearrow \propto f_{nl}$

## Short Summary

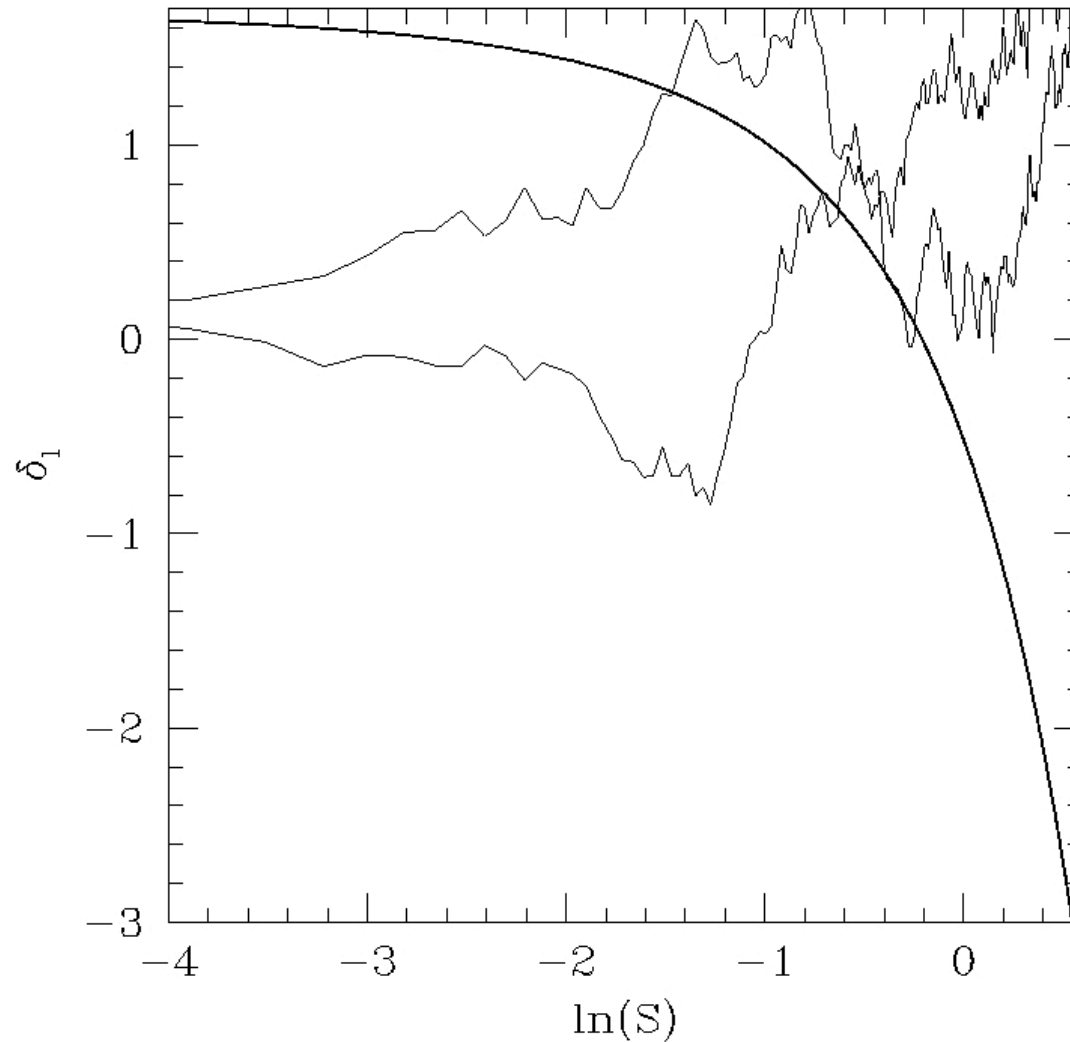
- \* Primordial non-Gaussianity changes the distribution of the initial perturbations, hence left signatures on LSS.
- \* Our analytical model describes the signature in the real space PDF accurately and was verified by comparing to N-body simulations.
- \* The modification in the nonlinear PDF is asymmetric: the effect of  $f_{nl}$  is stronger in underdense regions.
- \* The redshift space distortion is expected to have primordial non-Gaussianity signature -- the ellipsoidal collapse model is applied in this study.
- \* I extended the Doroshkevich formula on the distribution of the eigenvalues of the shear field to the local  $f_{nl}$  model -- other results with Gaussian initial conditions can be extended easily.
- \* The redshift space PDF is accurately described by this analytical model -- primordial non-Gaussianity left a signal in the redshift space distortion.

# Signature of primordial non-Gaussianity on LSS -- halo (& void) abundances

- \* Virialized dark matter halos are rare objects -- hence its distribution can probe the extremum of the matter distribution.
- \* Halo mass function is an important cosmological quantity -- can also constrain  $f_{\text{nl}}$ .
- \* Press & Schechter (1974) formalism: halos form from sufficiently overdense regions in the initial field  $\longrightarrow$  count the number of regions exceeding a critical value  $\delta_c$ .
- \* Lee & Shandarin (1998): halos form tri-axially  $\longrightarrow$  criteria for halo formation is  $\lambda_l > \lambda_c$

# Excursion set approach and cloud-in-cloud effect

- \* Both for  
account  
overde
- \* One sh  
scale, c  
Then g
- \* Excurs  
such co  
the rm
- \* The cr  
barrier  
**crossin**



effect into  
per

smoothing  
t density.

perform  
fact that  
ass.

ed by a  
ne **first**  
ed.

## Sheth-Tormen mass function

$$n(m) = \frac{\bar{\rho}}{m^2} \frac{\partial F}{\partial \ln \nu} \frac{d \ln \nu}{d \ln m} \quad \text{where } \nu \equiv \frac{\delta_c}{\sigma(m)}$$

\*  $\frac{\partial F}{\partial \ln \nu}$  denotes the first crossing probability.

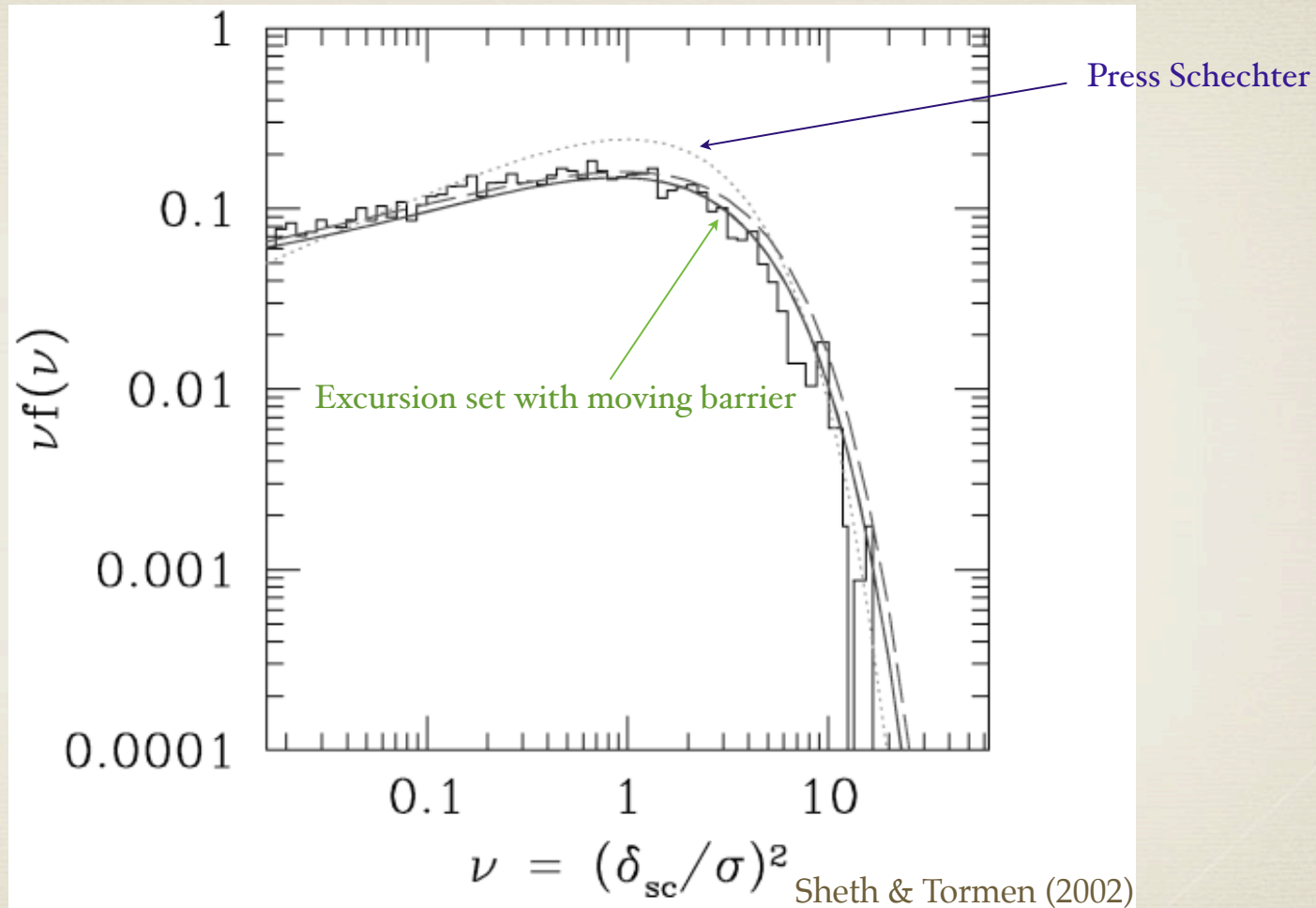
\* It can be obtained by either Monte-Carlo simulation or fitting formula.

\* Sheth & Tormen (2002) gave the following fitting formula:

$$f(S)dS = |T(S)| \exp \left[ -\frac{B(S)^2}{2S} \right] \frac{dS/S}{\sqrt{2\pi S}}$$

where  $T(S) = \sum_{n=0}^5 \frac{(-S)^n}{n!} \frac{\partial^n B}{\partial S^n}$ ,  $S = \sigma^2$ , and  $B(S)$  is the barrier

# Halo mass function for $f_{nl} = 0$



$$B(\sigma) = \sqrt{a}\delta_c [1 + \beta(\sigma/\sqrt{a}\delta_c)^{2\gamma}]$$

where  $a = 0.7$ ,  $\beta = 0.4$ , and  $\gamma = 0.6$ .

# Extension of excursion set approach to $f_{\text{nl}}$ model

- \* Lo Verde et al. (2008) and Matarrese et al. (2000) used the Press Schechter formalism to estimate the halo mass function when  $f_{\text{nl}}$  is non zero.
- \* They found that, even though the halo mass function from the PS formalism does not match the N-body simulations when the primordial perturbation is Gaussian, the ratio  $n(m, f_{\text{nl}})/n(m, f_{\text{nl}}=0)$  matches the measurements very well.
- \* Aim of our study: provide a consistent approach to study the change in the halo mass function when  $f_{\text{nl}}$  is non zero.
- \* It turns out that our approach reveals some information either missed and neglected by previous studies. It also clarifies the approximation formula given in Sheth & Tormen (2002).

## Excursion set approach in $f_{nl}$ model

- \* As shown earlier, the distributions of shape parameters are unchanged for a given linear overdensity.
- \* Hence the same barrier found in Sheth & Tormen (2002) can be used.
- \* However the first crossing probability across the same barrier  $B(S)$  is changed.
- \* Use the Edgeworth expansion and the bi-variate Edgeworth expansion to approximate the distributions  $p(\delta, s)$  and  $p(\delta_1, s | \delta_2, S)$

## First crossing probability across $B(S)$

$$p(\delta, s) = \int_0^s dS f(S, B(S)) p(\delta, s | B(S), S, \text{first}) \quad \text{for } \delta > B(S)$$

and

$$\begin{aligned} P(b, s) &= \int_{b(s)}^{\infty} d\delta p(\delta, s) \\ &= \int_0^s dS f(S, B) \int_b^{\infty} d\delta p(\delta, s | B, S, \text{first}) \end{aligned}$$

derivative wrt to  $s$  fields an integral equation of the first crossing distribution  $f(S, B)$

Case 1 --  $f_{nl} = 0$

\* The above argument leads to the following solution of the first crossing probability across a moving barrier:

$$s f_0(s, b) = \left[ b - s \frac{\partial b}{\partial s} \right] \frac{e^{-b^2/2s}}{\sqrt{2\pi s}} - \sum_{i=2}^{\infty} \frac{s^i}{i!} \frac{\partial^i b}{\partial s^i} \int_0^s dS f_0(S, B) \frac{e^{-(b-B)^2/2(s-S)}}{\sqrt{2\pi(s-S)}} (S/s - 1)^{i-1}$$

The approximation formula given in Sheth & Tormen (2002) corresponds to ignoring the  $S/s$  terms and keeping only the first few terms in the series.

## Case 2 -- $f_{nl} \neq 0$

- \* For non zero  $f_{nl}$ , the conditional probability is more complicated as  $p(\delta_1, s | \delta_2, S) \neq p(\delta_1 - \delta_2 | s - S)$
- \* Use bivariate Edgeworth expansion to approximate this conditional probability
- \* This ignores the correlation between steps and the fact that the walk did not cross  $\delta_2$  before  $S$

The resulting integral equation is

$$\frac{f_0(s, b)}{2} \left[ 1 + \frac{\sigma S_3}{6} H_3 \left( \frac{b}{\sqrt{s}} \right) \right] \leftarrow f^{(0)}(s, b)$$

$$= \frac{f(s, b)}{2} \left\{ 1 + 2 \int_0^s dS \frac{\partial}{\partial s} P_0 \left( \frac{b-B}{\sqrt{s-S}} \right) \frac{f(S, B) - f_0(S, B) [1 + (\sigma S_3/6) H_3(b/\sqrt{s})]}{f(s, b)} \right.$$

$$\left. + 2 \frac{\sigma S_3}{6} \int_0^s dS \frac{f(S, B)}{f(s, b)} \frac{\partial}{\partial s} \left[ \mathcal{E}(s, S) p_0 \left( \frac{b-B}{\sqrt{s-S}} \right) \right] \right\}.$$

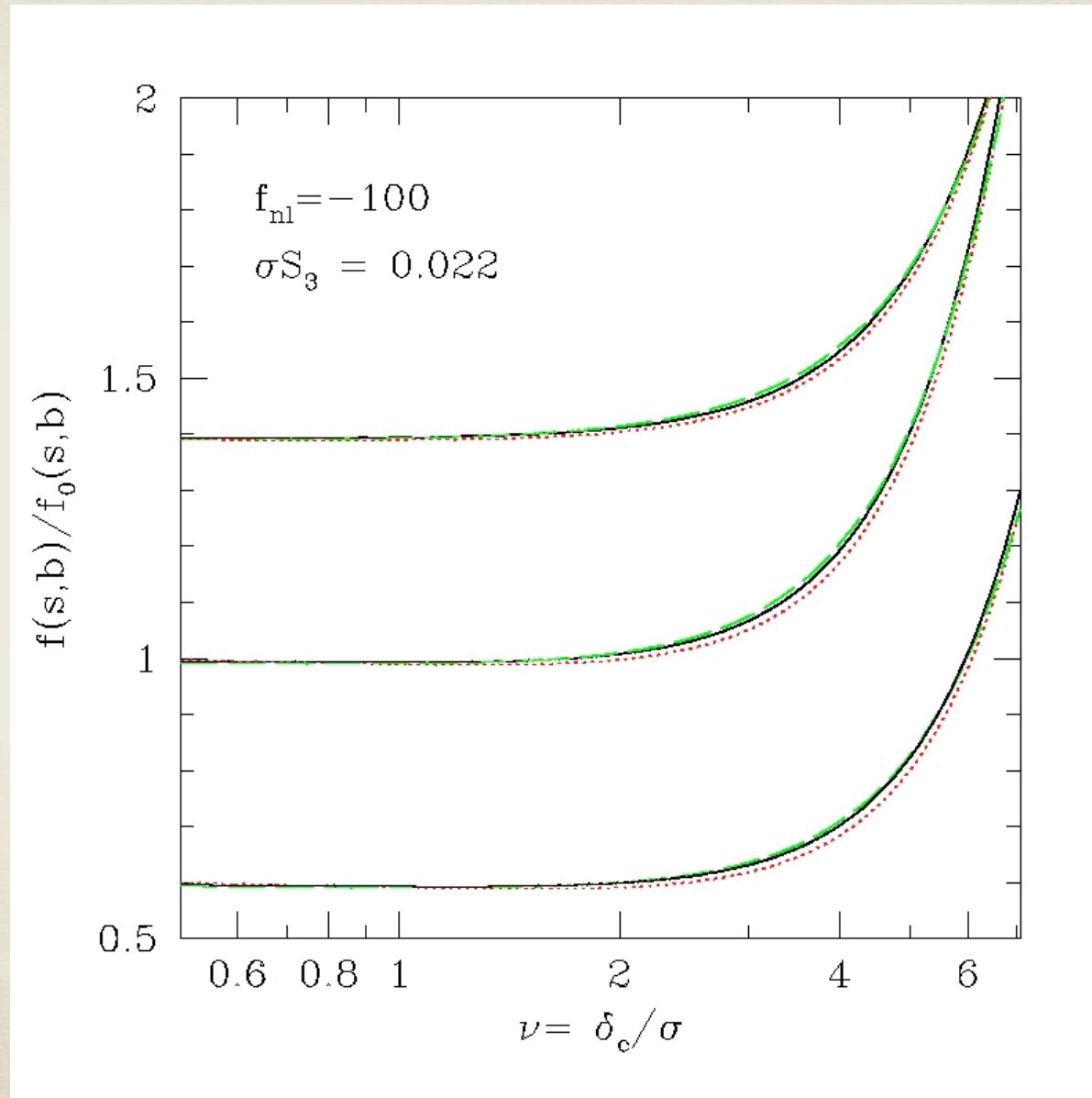
Keeping terms to the first order of  $\sigma S_3$

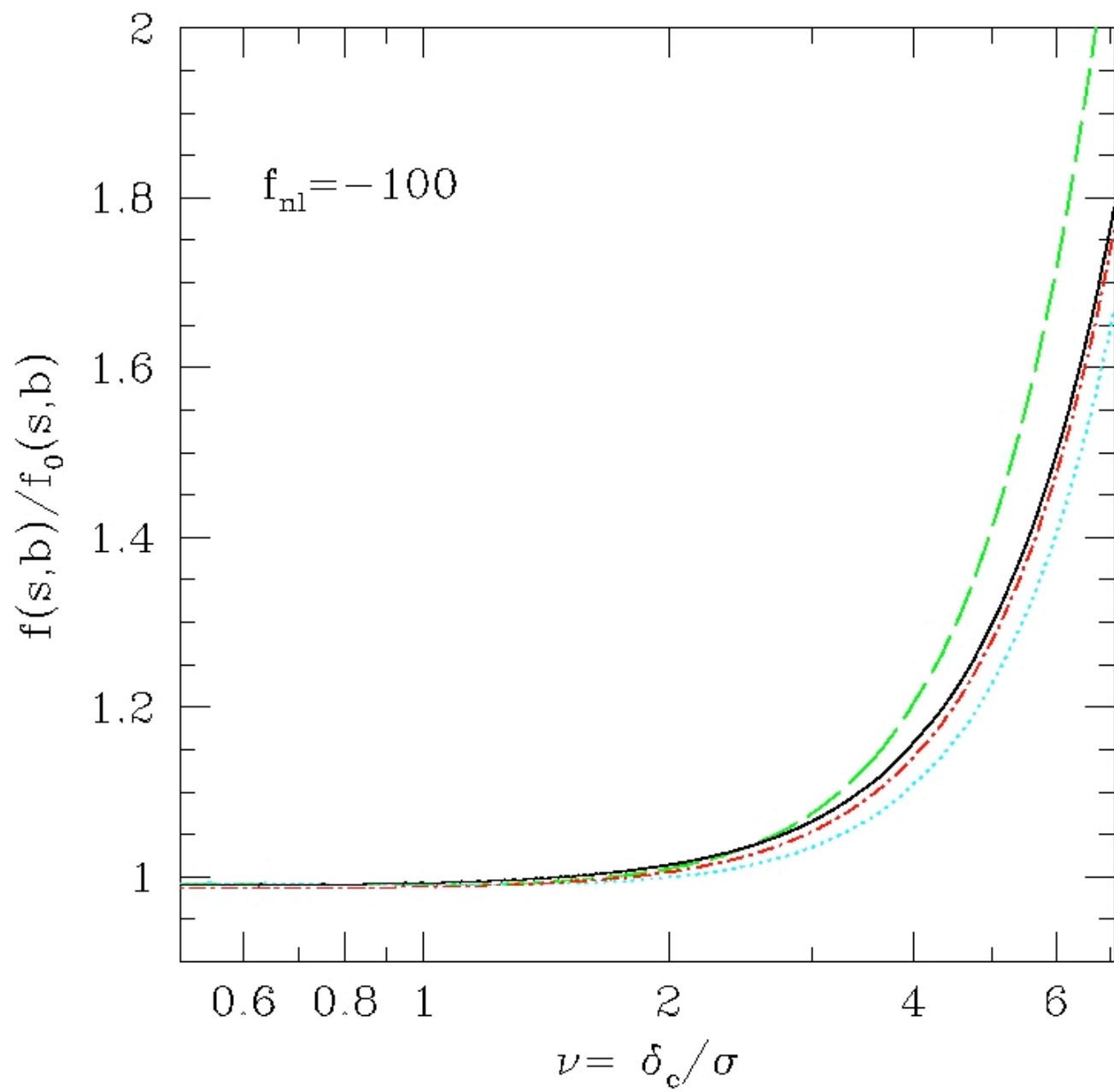
$$f(s, b) = f^{(0)}(s, b) \left( 1 + \frac{f^{(1)}}{f^{(0)}} \right) \approx f_0(s, b) \left[ 1 + \frac{\sigma S_3}{6} H_3 \left( \frac{b}{\sqrt{s}} \right) - \frac{\sigma S_3}{6} \mathcal{G}(s) \right]$$

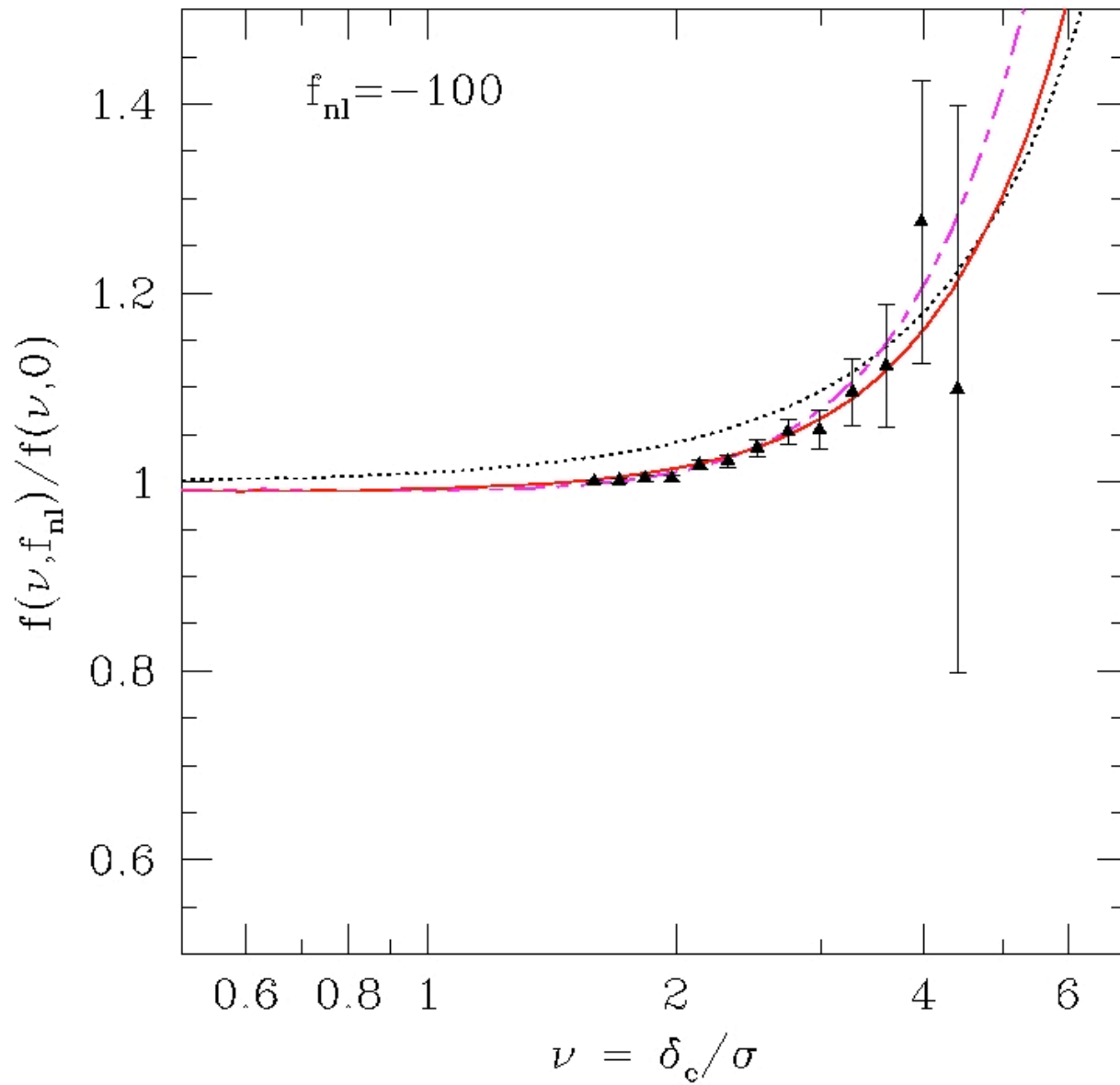
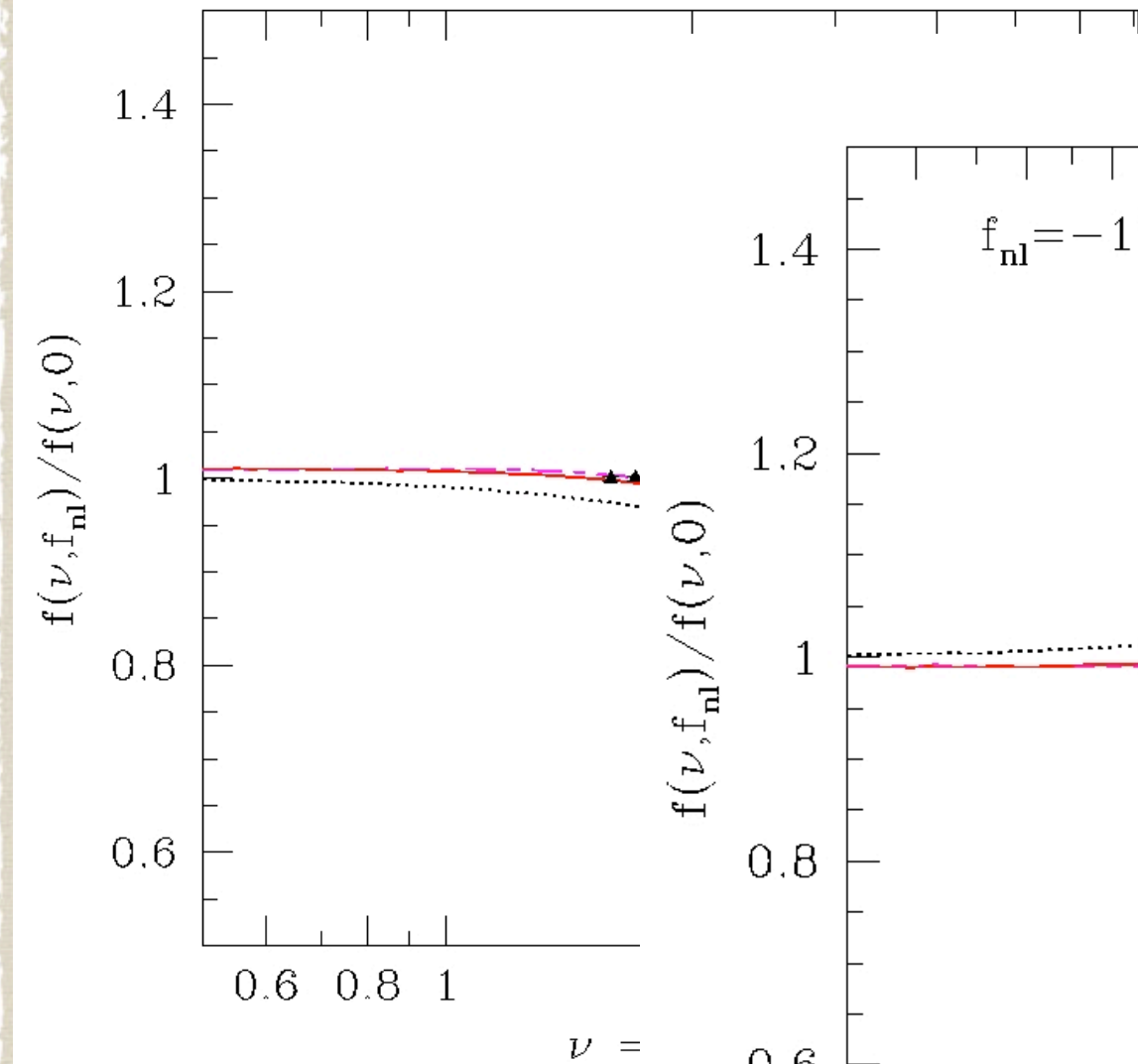
where  $\mathcal{G}(s)$  is a complicated function depending on the barrier and the first crossing distribution for  $f_{nl} \neq 0$

**and it is non zero for constant barrier**

- \* Previous studies either explicitly neglected (Matarrese et al. 2000) or missed (LoVerde et al. 2008) this term.







## Short Summary (on halo mass function)

- \* extension of the excursion set approach to the local  $f_{nl}$  model yields an extra term that is either missed or neglected in earlier studies;
- \* this term turns out to be small: it explains why earlier studies match N-body measurements without this term;
- \* however, our approach is the only consistent approach that can match the ratio change when comparing the halo mass function  $n(m, f_{nl})/n(m, f_{nl}=0)$
- \* as well as the halo mass function when  $f_{nl}=0$ ;
- \* it also explains an approximation formula given in Sheth & Tormen (2002)

## Void abundances in local $f_{nl}$ model

- \* Primordial non-Gaussianity modifies the tails of the PDF of the dark matter field;
- \* the signature in the underdense region is stronger;
- \* hence, in addition to halo mass function, void abundances can also probe primordial non-Gaussianity;
- \* the excursion set formalism can be used to study the void abundances -- includes both the cloud-in-cloud AND the void-in-cloud effect

## Void-in-Cloud effect

- \* Unlike halos, which can reside in underdense region, voids cannot sit inside a halo  $\longrightarrow$  void-in-cloud effect;
- \* In the excursion set language, it is a two-barrier problem ( $\delta_c$  for halo formation,  $\delta_v$  for void);
- \* want to count: all first crossings across the void barrier, without crossing the halo barrier at smaller  $s$  (more massive scale);

## Excursion set approach: 2 barrier problem

$$\mathcal{F}(s, \delta_v, \delta_c) = f(s, \delta_v) - \int_0^s dS_1 \mathcal{F}(S_1, \delta_c, \delta_v) f(s, \delta_v | S_1, \delta_c)$$

Probability of crossing  $\delta_v$  at  $s$ , but did not cross  $\delta_c$

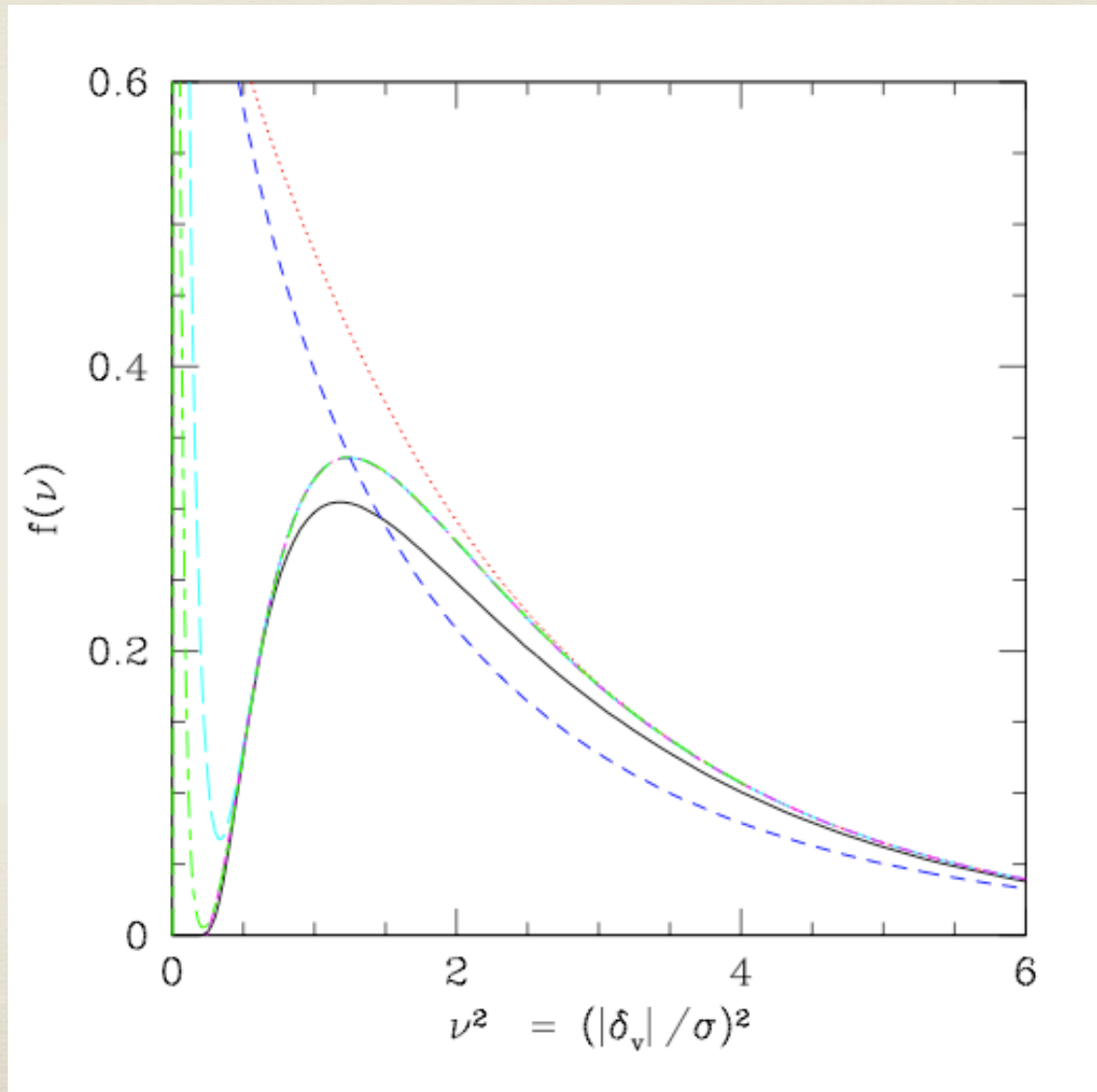
Swapping  $\delta_v$  and  $\delta_c$  

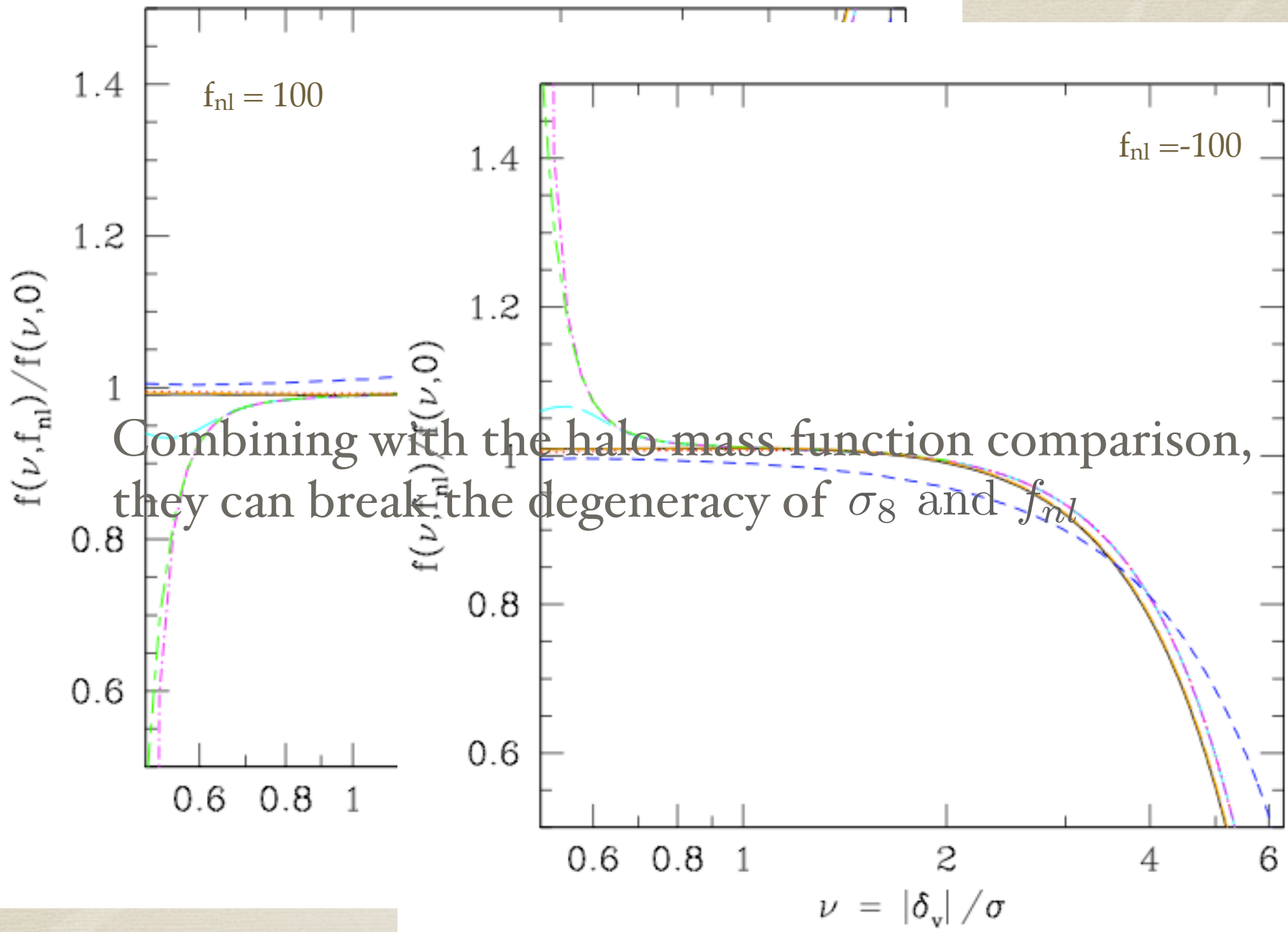
Recurrence relation between  $\mathcal{F}$  and  $f$

$$\mathcal{F}(s, \delta_v, \delta_c) = f(s, \delta_v) + \sum_{n=1}^{\infty} (-1)^n \int_0^{S_0} dS_1 \dots \int_0^{S_{n-1}} dS_n \prod_{m=0}^{n-1} f(S_m, \delta_m | S_{m+1}, \delta_{m+1}) f(S_n, \delta_n)$$

where  $S_0 \equiv s$ ,  $\delta_n = \delta_v$  (n even) or  $\delta_c$  (n odd)

# Void Abundances when $f_{nl} = 0$





Combining with the halo mass function comparison, they can break the degeneracy of  $\sigma_8$  and  $f_{nl}$

# Conclusions

- \* Primordial non-Gaussianity is of much recent attractions due to its ability to distinguish inflation models;
- \* LSS can be used a probe to primordial non-Gaussianity: this is complementary to the CMB constraints;
- \* In this talk we look at 4 different probes: PDF of dark matter field, redshift space distortion, halo mass function & void abundances;
- \* Future work: combining these methods with other LSS probes to tighten constraints;
- \* Extension to other primordial non-Gaussianity models